

# **Development and Testing of Hydrogen Storage System(s) for Capturing Intermittent Renewable Energy Sources for Peak Demand Utilization on the Grid**

**Prepared for the**

**U.S. Department of Energy  
Office of Electricity Delivery and Energy Reliability**

**Under Award No. DE-FC-06NT42847  
Task 2.2. Deliverable #1 –  
Analysis of Test Results for Hydrogen Storage Systems**

**By**

**Hawaii Natural Energy Institute  
School of Ocean and Earth Science and Technology  
University of Hawaii**

**May 2008**

*Acknowledgement:* This material is based upon work supported by the United States Department of Energy under Award Number DE-FC-06NT42847.

*Disclaimer:* This report was prepared as an account of work sponsored by an agency of the United States Government. Neither the United States Government nor any agency thereof, nor any of their employees, makes any warranty, express or implied, or assumes any legal liability or responsibility for the accuracy, completeness, or usefulness of any information, apparatus, product, or process disclosed, or represents that its use would not infringe privately owned rights. Reference herein to any specific commercial product, process, or service by trade name, trademark, manufacturer, or otherwise does not necessarily constitute or imply its endorsement, recommendation, or favoring by the United States Government or any agency thereof. The views and opinions of authors expressed herein do not necessarily state or reflect those of the United States Government or any agency thereof.

# Table of Contents

<u>Section Number and Title</u>	<u>Page Number</u>
1 Introduction	1
2 Description of the Electrochemical Components	1
2.1 PEM Electrolyzer System Supplied by Electric Hydrogen	2
2.2 5 kW PEM Fuel Cell System Supplied by Plug Power	2
3 Performance Evaluation of Kahua Ranch Hydrogen Storage System	3
3.1 Kahua Ranch Power System	3
3.2 Electrolyzer Experimental Results	3
3.3 Fuel Cell Systems Experimental Results	5
3.4 Performance Evaluation of Kahua's HSS	7
4 Conclusions	8
4.1 Electrolyzer Performance	8
4.2 Fuel Cell Performance	8
4.3 System Optimization	8
5 Discussion of Results	8
5.1 Advantages of HSS Systems	8

5.2	Hydrogen System Efficiency	9
5.3	Renewable Energy Hydrogen Production Systems	9
6	References	10
Annex A	Analysis Approach of the Electrochemical Components – Steady-State Operation	11

# **Development and Testing of Hydrogen Storage System(s) for Capturing Intermittent Renewable Energy Sources for Peak Demand Utilization on the Grid**

## **1. Introduction**

As part of the Hawaii Distributed Energy Resource Technologies for Energy Security Program, the Hawaii Natural Energy Institute (HNEI) installed, tested, evaluated, and demonstrated integrated systems for the production of hydrogen from renewable energy resources. This effort was originally planned for implementation at the Hawaii Gateway Energy Center (HGEC), located at the Natural Energy Laboratory of Hawaii Authority (NELHA) on the Big Island; however, Kahua Ranch, also located in the Big Island, was selected to host this effort. There were a number of reasons for doing this - Kahua Ranch owners have worked for several years with the Pacific International Center for High Technology Research (PICHTR) to obtain funding from the Japanese government's Ministry of Foreign Affairs (MOFA) to test, demonstrate, and deploy renewable energy systems to Pacific Island Nations. As a result of these efforts (which included cost share from PICHTR and Japan), considerable infrastructure already existed at Kahua comprised of photovoltaic (PV), wind turbine (WT), battery, and electrical distribution infrastructure systems which are not available at HGEC. This effort also leveraged major system components, such as the fuel cell, electrolyzer, and data acquisition systems, which were purchased and tested under a previous program.

This facility demonstrated one example of a hydrogen storage system (HSS) consisting of an electrolyzer, hydrogen storage, and fuel cell. This system is capable of remote operation with data acquisition and control over the internet. The following is a discussion of some of the experimental results that have been derived from the operation of this new and upgraded facility. Based on these experimental data, some additional observations and conclusions can be drawn concerning integrated hydrogen systems. These initial observations are important, since this facility is one of the few in the world that is now producing renewable hydrogen for use in fuel cells and transportation systems.

## **2. Description of the Electrochemical Components**

The layout of the Kahua Ranch system is illustrated in Figure 1. The major HSS hydrogen equipment components installed at Kahua are commercially available, low-production-volume units. The PEM fuel cell system represents the latest in advances in the industry and was designed as an uninterruptible power supply (UPS) capable of load following. The electrolyzer is a PEM prototype developed by Electric Hydrogen for our stand-alone application in terms of power and operation, and is optimized for fast start-up and variable power input that is characteristic of wind and PV power generation systems.

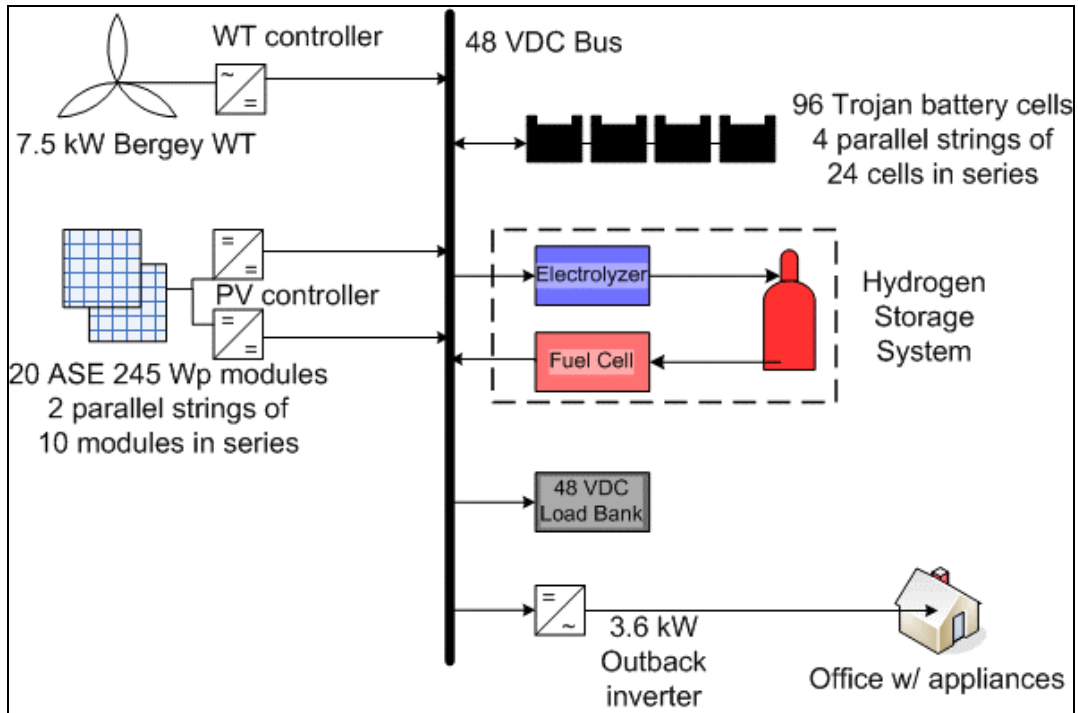


Figure 1: Kahua Ranch System Layout

### 2.1 PEM Electrolyzer System supplied by Electric Hydrogen

The PEM electrolyzer produces 0.2 Nm<sup>3</sup>/h of hydrogen at 12 bar. The electrical input specifications are: 25 A at 48 VDC battery voltage range or 46 V to 58 V. A converter converts incoming DC power to properly supply the cell stack. The system is supplied with deionized water (ASTM Type I), at a maximum rate of 1 liter per minute and pressure between 0.2 bar and 1.4 bar (3-20 psi).

The electrolyzer system consists of a gas generation unit, a gas/liquid management unit, and a cooling unit. The gas generation unit contains a stack of PEM cells connected in series. The stack is mechanically connected on the cathode side to the gas/liquid separator and a pressure regulator, allowing hydrogen production upon reaching 12 bar. The anode side of the stack is connected to a gas/liquid tank for drying oxygen and managing the water level in the stack. The product oxygen is vented to atmosphere. A solenoid valve allows water to fill up the tank when reaching a preset low water level. The cooling unit, part of the anode side, contains a water pump and an air/liquid heat exchanger to regulate stack temperature. Finally, the unit is protected by an outdoor-capable cabinet that is vented in order to cool the unit and to avoid hydrogen accumulation. An integrated hydrogen sensor in the cabinet shuts down the unit if hydrogen is detected.

### 2.2 5 kW PEM Fuel Cell System Supplied by Plug Power

The fuel cell system requires pure hydrogen (99.95%, dry), access to ambient air (temperature between -40 °C to 46 °C and non-condensing relative humidity between

0% to 95%), and produces regulated 48 VDC electrical power. The outputs are oxygen-depleted humidified air and liquid water.

The system consists of a stack of cells connected in series, air and hydrogen supply units, a cooling unit, a power converter, a battery pack wired in parallel with the fuel cell system output, and a microprocessor for data acquisition and automatic operation. The hydrogen supply system includes an exhaust gas recirculation system for injecting non-consumed hydrogen and water vapor into the anode inlet stream. There is no active hydrogen flow controller; instead, hydrogen automatically enters the system through a pressure regulator to maintain 0.07 bar (gauge) into the gas line. The air supply unit consists of a filter that removes hydrocarbons and other chemicals, an air blower with speed mapped to fuel cell power demand, and a humidifier. The cooling unit has a single-speed circulation pump and two coolant loops. One loop includes a heater used at start-up to heat the stack to the operating temperature of approximately 55 °C. The second loop is used for cooling the stack by passing the coolant through a radiator, which has a fan with speed mapped to fuel cell power demand.

The batteries are used at start-up to supply auxiliary power; however, as soon as the fuel cell is connected to the DC bus, the stack supplies power to the parasitic loads. The power converters use either the stack power or the battery power to support the load with regulated voltage between 46 V and 56 V.

### **3. Performance Evaluation of Kahua Ranch Hydrogen Storage System**

#### **3.1 Kahua Ranch Power System**

The Kahua Ranch Power System has been designed as a stand-alone power system which includes: 1) renewable energy resource generators comprised of a wind turbine generator (WTG), 2) a photovoltaic array (PV), 3) a lead-acid battery as short-term electricity storage, and 4) a hydrogen storage system for long-term energy storage, consisting of an electrolyzer, a low pressure (175 psi) hydrogen gas storage system, and a fuel cell. Within this system, hydrogen is supplied to the 5 kW fuel cell power system that then provides 48 VDC power to the 48 VDC main electrical bus bar.

The stand-alone operation mode allows automatic start-up/shut-down of each component connected to the common 48 VDC bus bar. The operating rules programmed in a central controller using LabVIEW software are: 1) the load is the priority load, 2) all excess RE generation is stored first into the battery storage and then into hydrogen by supplying the electrolyzer, and 3) in case of a deficit of RE supply compared to the load, the batteries help match the load and if necessary the FC also supplies the load. The complete installation is effectively controlled by tracking the bus bar voltage and the hydrogen gas storage pressure.

#### **3.2 Electrolyzer Experimental Results**

The analysis here is based on the higher heating value (HHV) of hydrogen. The analysis approach is described in Annex A. Figure 2 shows the time evolution of the

main electrolyzer data on long-term operation tests: 1) unit current and voltage, 2) hydrogen flow, and 3) calculated electrolyzer efficiency, based on the Higher Heating Value (HHV) of hydrogen. When the unit was started at 8:40 am, the unit current increased to 35 A in 18 minutes. This high current operation helped in reaching optimal operating conditions. Following this warm-up period, the current dropped down to 25 A, reaching its optimal operating point at 10 am. Only 2.5 minutes are necessary for the unit to deliver hydrogen after supplying electricity to the electrolyzer stack. At the optimal operating point, the average flow was 3.5 SLM (0.2 Nm<sup>3</sup>/h). The unit current averaged 25 A at 55 V. The efficiency of the electrolyzer at the optimal operating point was 50.2% (HHV), equivalent to an energy consumption of 7 kWh/Nm<sup>3</sup>. This operation mode is close to the steady-state operation results. The performance of the PEM electrolyzer is thus equivalent to the 6 Nm<sup>3</sup>/h alkaline electrolyzer, but the warm-up period is significantly shorter thanks to the small size and the design of the PEM unit.

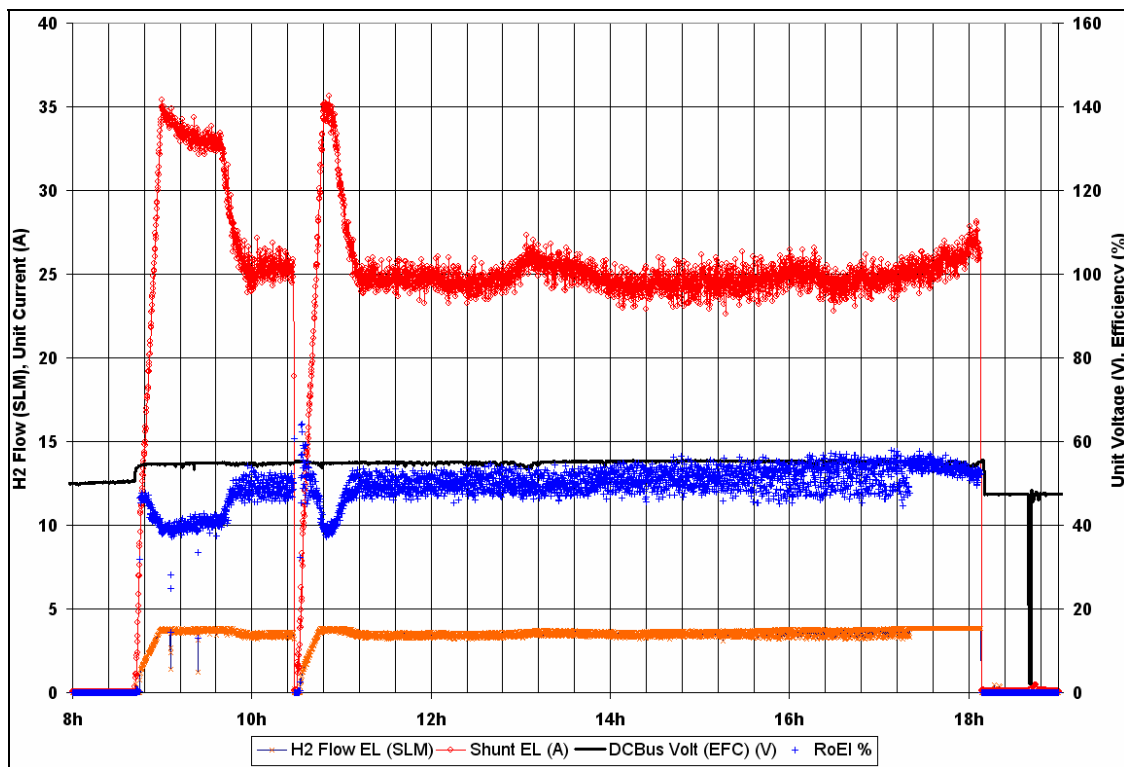


**Figure 2: Electrolyzer data evolution versus time: Current and voltage of the unit, hydrogen production flow and efficiency (HHV) – December 21<sup>st</sup>, 2007.**

This steady-state operation mode does not always occur when integrated into the complete Kahua Ranch installation.

Figure 3 shows the main data of the electrolyzer in stand-alone operation in the complete power system. The electrolyzer operates for either short or long periods of time, depending on the renewable resource availability. The shortest period was 10 minutes (on December 22<sup>nd</sup> at 6 am), where the current did not even reach its optimal operating point. The longest period was about 5

hours. The brown line on Figure 3 is the pressure in the hydrogen storage (320 liters). When the pressure reached its maximum pressure, set at 165 psi, the electrolyzer was disconnected by the central controller. The overall energy needed to fill up the storage, equivalent to 2.75 Nm<sup>3</sup> of hydrogen (HHV), was calculated at 21.4 kWh. The efficiency of the electrolyzer in operation in the complete installation was then equal to 7.8 kWh/Nm<sup>3</sup> or 45.4% (HHV) only 5% less than the similarly steady-state operation performance.

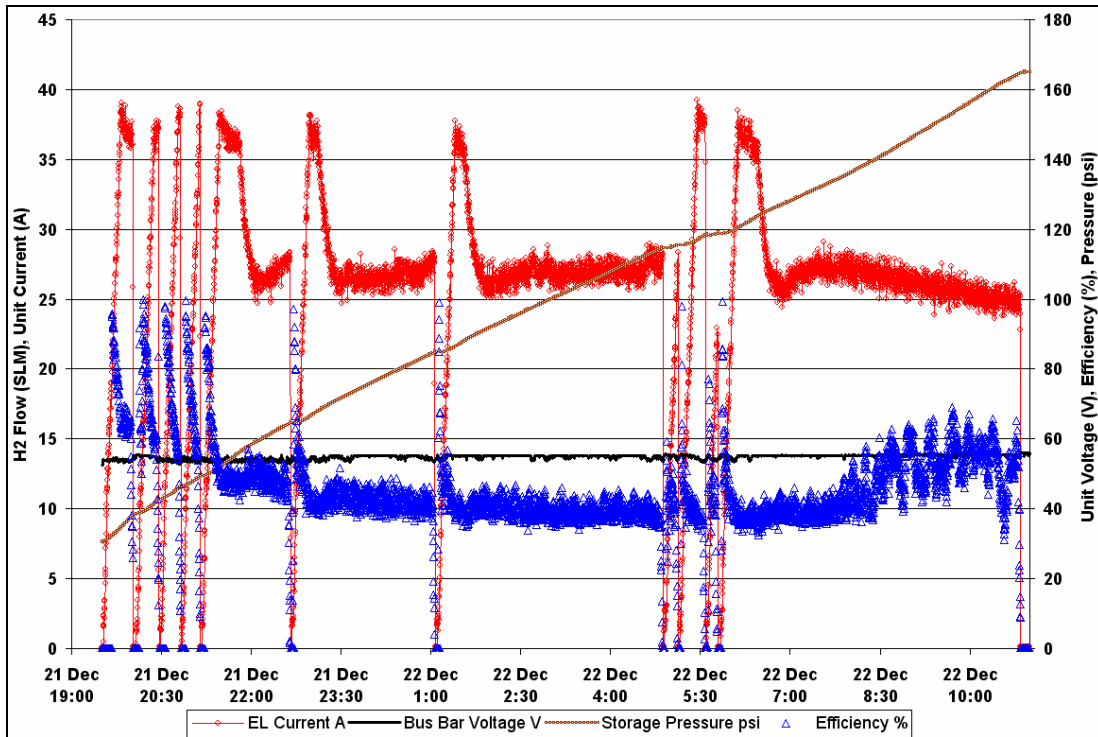


Figure 3: Electrolyzer data in stand-alone operation mode for the complete installation.

### 3.3 Fuel Cell System Experimental Results

The fuel cell (FC) system is used to supply the load when the renewable energy availability is low and the battery storage is empty. The bus voltage is used to evaluate the state of charge (SOC) of the battery storage unit. The FC unit has a low-bus-voltage operation mode. It has been set to start operation when the bus voltage reaches its low value (47 V). It automatically shuts down when the bus voltage is higher than 47.7 V.

Figure 4 shows the FC operation on November 17<sup>th</sup>, 2007 when only the photovoltaic array was connected to the bus bar and the load demand was constant equal to 133 A. The light blue stars correspond to the PV current varying from 2 A to 42 A as a function of the solar radiation. The black circles are the bus voltage data. Just before 13:40, the voltage reached 47 V and the FC started. The FC current is negative for a short period

at the start-up, allowing the auxiliaries to be supplied. The stack is in operation shortly after and the FC current unit is positive. The hydrogen flow increased drastically at the start-up and was then proportional to the unit current. Until time 13:55, the FC heater was on, in order to quickly reach the optimal temperature. During this start-up period, the FC unit efficiency, calculated using the power produced by the FC system divided by the power equivalent to hydrogen consumption (HHV), is between 12% and 27%. Then the FC unit efficiency is between 28% and 35%. Out-of-range efficiencies are due to the transient behavior of the FC unit using its batteries to soften the necessary variation of the stack production to supply the load demand. During the entire operation, the FC unit current varied from 0 A to 42 A to match the load in addition to the PV and the batteries whose current was between 50 A and 100 A. Just after time 15:00, the hydrogen storage reached the low pressure level and the load was disconnected from the bus-bar by the controller to avoid the FC unit running out of hydrogen. The load disconnection is followed by a drastic increase of the bus-bar voltage up to 49 V signaling the FC unit to shut down.

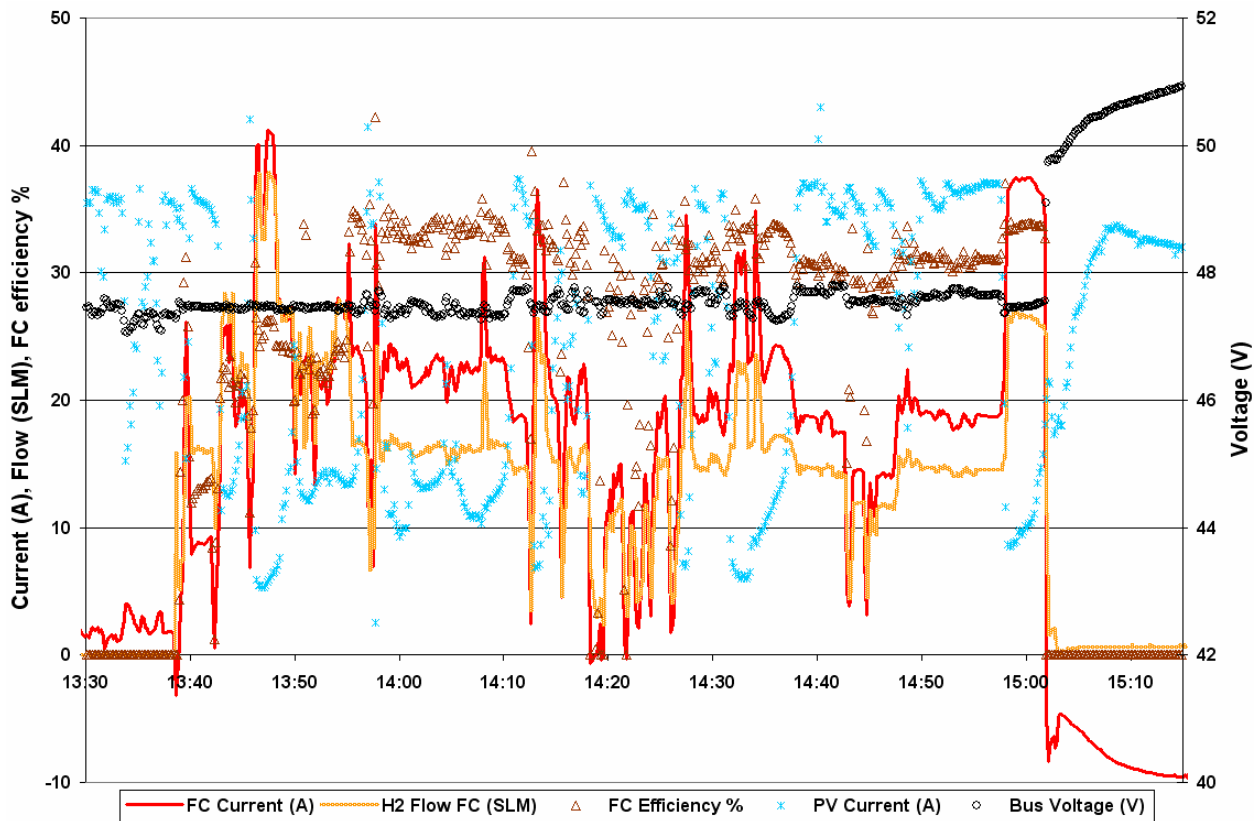


Figure 4: FC unit operation in the complete installation – November 17<sup>th</sup> 2007.

Figure 5 shows the efficiency of the FC unit in operation in the complete installation as a function of the electrical output power. The crosses are the points recorded on November 17<sup>th</sup>, 2007. The diamond (or rhombus) points have been recorded when the FC unit was directly supplying the load in order to reach higher power demand. FC

system efficiency primarily ranges between 28% and 40%, and above 35% for power levels higher than 3.5 kW. The low efficiency points below 30% correspond to the warm-up period performance. Compared to the steady-state operation mode recorded in 2005, the real-time efficiency is disparate and mainly lower. This is due to the transient behavior of the unit using its included batteries to match the load demand. Moreover, the short operation time and the variable load demands in the complete power system did not allow the FC unit to reach optimal operating conditions.

In addition, although it is convenient to have a 5 kW FC unit to help supply the load demand, the operation in parallel with a large battery storage capacity would require a less powerful FC unit. This would allow higher system efficiency.

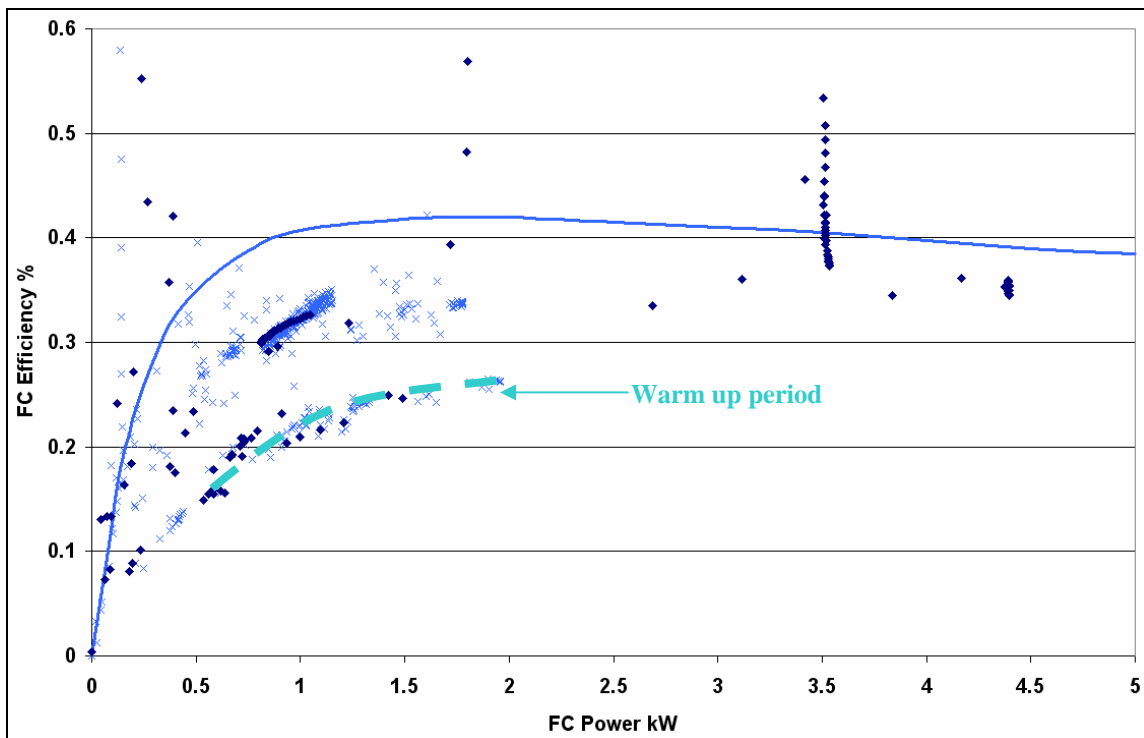


Figure 5: FC efficiency (HHV) as a function of electrical output power.

### 3.4 Performance Evaluation of Kahua's HSS

Results on overall system operation recorded over 68 days of stand-alone operation demonstrated an average efficiency of the Kahua HSS at between 12% and 17%. This efficiency of the HSS is in agreement with the component efficiency in stand-alone operation: around 45% for the electrolyzer and between 30% and 40% for the FC.

## 4. Conclusions

### 4.1 Electrolyzer Performance

The electrolyzer shows an energy consumption of about 7 kWh/Nm<sup>3</sup> in steady-state operation, corresponding to the present state-of-the-art. A major advantage of the PEM unit is the very short warm-up period allowing good performance even when integrated into a power system. More experimentation is required to localize potential performance improvement areas.

### 4.2 Fuel Cell Performance

The tests made on the 5 kW FC unit show that the unit has reasonable efficiency over most of its power range. Improvements in stack performance and the auxiliaries are the main keys for higher unit efficiency. In operation in an intermittent RE power system, the unit is 5% to 10% less efficient. This causes the HSS to reach 12% to 17% efficiency in operation in the RE power system instead of 19% to 24% in steady-state operation.

### 4.3 System Optimization

These results prove that electrochemical system components must be carefully optimized in order to reach higher system efficiency. Steady-state performance should be optimized by reducing any loss in the stack and in the auxiliaries. Higher efficiency auxiliaries as well as waste heat recovery would lead to much higher performances. In addition, warm-up periods should be shortened as much as possible when integrated into an intermittent RE power system.

## 5. Discussion of Results

### 5.1 Advantages of HSS Systems

Looking at the reported results, there are significant technical and economic challenges for the production of hydrogen from electrolysis to store energy. Important improvements are necessary to reach better efficiency and lower costs; however, there are value-added advantages of the HSS that are important and unique that should be considered and evaluated:

- Hydrogen is an environmentally friendly energy carrier:  
When using hydrogen produced by an electrolyzer that is powered by a renewable energy source, the only by-product of a fuel cell or an internal combustion engine (ICE) is water, although an ICE might produce low levels of NO<sub>x</sub> under some operating conditions. The water then returns to nature's cycle and can be split again into hydrogen.
- Long-Term Seasonal Storage:  
Storing hydrogen gas allows long-term storage with almost no loss over time. The first experiments on renewable hydrogen systems in the nineties demonstrated the potential of using hydrogen for seasonal storage to store

from summer to winter, advantages only available when using pumped hydro or compressed air storage technologies.

- *Utilization of Hydrogen for Transportation:*  
This experiment demonstrated the use of hydrogen to support the use of intermittent renewable energy sources for firm power electrical applications. The hydrogen can also be used to supply other applications such as transportation.
- *Combined Heat and Power:*  
As identified in the first parts of this document, electrolyzers and fuel cells should have a design allowing for the capture and use of waste heat. In addition to much higher system efficiency, heat is an important by-product in some market niches, especially when supplying homes in remote areas.
- *Decoupling Power Production from Energy Storage*  
Hydrogen storage allows for the independent sizing of energy and power, contrary to batteries (except flow batteries). Each part of the HSS is independent of the others. Therefore, the electrolyzer is sized to match the available excess of energy or the required flow. The FC power is selected to match the load or the maximum required power demand. In addition, electrolyzers and fuel cells have a very wide power range. Finally, the gas volume depends on the needs of the stored energy and on the efficiency of the FC unit, the ICE, or any other components converting hydrogen to the end-user energy requirement.

## **5.2. Hydrogen System Efficiency**

Previous studies have given results or predictions on hydrogen system efficiencies. The Finnish project NEMO in 1989, reached an HSS efficiency of 28% in operation in a 1.3 kW stand-alone operation [1]. The German Oldenburg project in 1990 discussed reaching a 50% efficient HSS [2]. Both of the studies addressed alkaline technologies and the main technical paths were focused on reducing auxiliary system parasitic consumption. PEM technologies require simpler peripherals and eliminate the use of highly corrosive electrolyte, thus reducing auxiliary electrolyte management system power consumption. On the other hand, the PEM systems need to reach higher efficiency, longer life time, and lower cost. Our experimental efficiency results presented earlier are lower than alkaline technologies, especially due to lower stack efficiency. Moreover, the tested components are pre-commercial units, a step further towards commercialized components, compared to the laboratory components of the older projects.

## **5.3. Renewable Energy Hydrogen Production Systems**

Although hydrogen storage systems have demonstrated relatively low potential efficiency (28% to be compared to the 75% to 85% round trip efficiency of batteries or pumped hydro storage solutions), the HSS advantages demonstrate good potential performance when integrated into RE power systems. Indeed, the long-term storage

capacity makes possible a perfect sizing of the installation. By using most of the RE generator production, the performance of the RE-H<sub>2</sub> power systems reached an efficiency of 44% (Fraunhofer, [3]) or 54% (PHOEBUS, [4]) with a potential efficiency of 65%. These results did not consider the possibility of utilizing heat generation. These performances are in the range of the RE-battery systems, being generally 30%-40% efficient due to the need of oversized RE generators [5].

Although it is necessary to resolve numerous technical challenges, hydrogen is definitely a very good storage solution for RE generators, especially in applications requiring long-term energy storage and heat generation. Development of hydrogen fueled vehicles will increase the advantages of the HSS. Developers of hydrogen technology components are presently focusing on cost reduction and reliability. The results presented in this report demonstrate that component efficiency is crucial, especially when an HSS is integrated into RE systems.

## 6. References

- [1] J.P. Vanhanen, "Operating experiences on a self-sufficient solar-H<sub>2</sub>-FC system," Proceedings of the 2<sup>nd</sup> Nordic Symposium on Hydrogen and Fuel cells for Energy Storage, pp. 46-54, Helsinki, Finland, 1995.
- [2] A. Haas & al., "Hydrogen energy storage for an autonomous renewable energy system – Analysis of experimental results," Proceedings of the ISES 1991 Solar World Congress, pp. 723-728, Denvers, Colorado, 1991.
- [3] A. Goetzberger & al., "The PV/Hydrogen/Oxygen – system of the self-sufficient solar house Freiburg," IEEE, pp. 1152-1158, 1993.
- [4] C. Meurer & al., "PHOEBUS – An autonomous supply system with renewable energy : six years of operational experience and advanced concepts," Solar Energy, Vol.67, N°1-3, pp. 131-138, 1999.
- [5] D. Mayer, M. Heidenreich, "Performance analysis of stand alone PV systems from a rational use of energy point of view," Proceeding of the 16<sup>th</sup> European Photovoltaic Solar Energy Conference, Glasgow, UK, May 2000, Poster VD2.28.

## Annex A

### Analysis Approach of the Electrochemical Components – Steady-State Operation

The enthalpy of liquid water formation (HHV) has been chosen as the basis of performance analysis. This choice allows for consistent comparisons between technologies, and presents the most appropriate basis for analysis of thermal losses, given low temperature operation of the electrochemical components.

The steady-state energy balance of the electrolyzer system is presented as Figure A. 1. The electrolyzer system is supplied with AC power,  $P_{elec}$ , which is used to power the auxiliaries, is consumed in the rectifier, and is converted into hydrogen and oxygen by the stack. The power consumed by the stack,  $P_{Stack}$ , is calculated by measuring the stack current and voltage. Based on these two measurements and the output hydrogen flow measurement, two other losses are calculated: the gas loss ( $P_{GL}$ ) and the thermal loss ( $P_{TL}$ ). Figure A. 2.a gives a graphical representation of how to evaluate these two power losses and Table A. 1 defines the efficiency terms used in this report. The thermal loss (top rectangle on Figure A. 2.a) of the stack can be calculated by multiplying the stack current by the difference between the measured stack voltage and the voltage corresponding to the higher heating value (HHV) of the reaction. Below this rectangle, the area corresponds to hydrogen power that could be theoretically produced by the stack. Knowing the actual hydrogen production rate, the real available hydrogen power is calculated as described by equation (1). Furthermore, the current equivalent to the real hydrogen flow,  $I_{eq}$ , is defined in equation (2). The difference between the actual current,  $I_{Stack}$ , and the current equivalent gives the amount of current that was consumed to produce the gas that was lost. Figure A. 1.a schematically shows the areas corresponding to the real hydrogen output power available for the end-user ( $P_{H_2}$ ) and the gas loss power ( $P_{GL}$ ), which includes gas recombination in the stack as well as gas loss in the process (e.g., leaks and venting to atmosphere for process pressure control).

$$P_{H_2} = \dot{n}_{H_2} \times HHV \quad (1)$$

$$I_{eq} = \frac{2 \times F}{N_{cell}} \times \dot{n}_{H_2} \quad (2)$$

where

- $P_{H_2}$  = Hydrogen power (W),
- $\dot{n}_{H_2}$  = Hydrogen molar flow ( $\text{mol}\cdot\text{s}^{-1}$ ),
- HHV = High heating value ( $285,830 \text{ J}\cdot\text{mol}^{-1}$ ),
- $I_{eq}$  = Current equivalent to the real hydrogen flow (A),
- F = Faraday number ( $96,485 \text{ C}\cdot\text{mol}^{-1}$ ), and
- $N_{cell}$  = Number of cells.

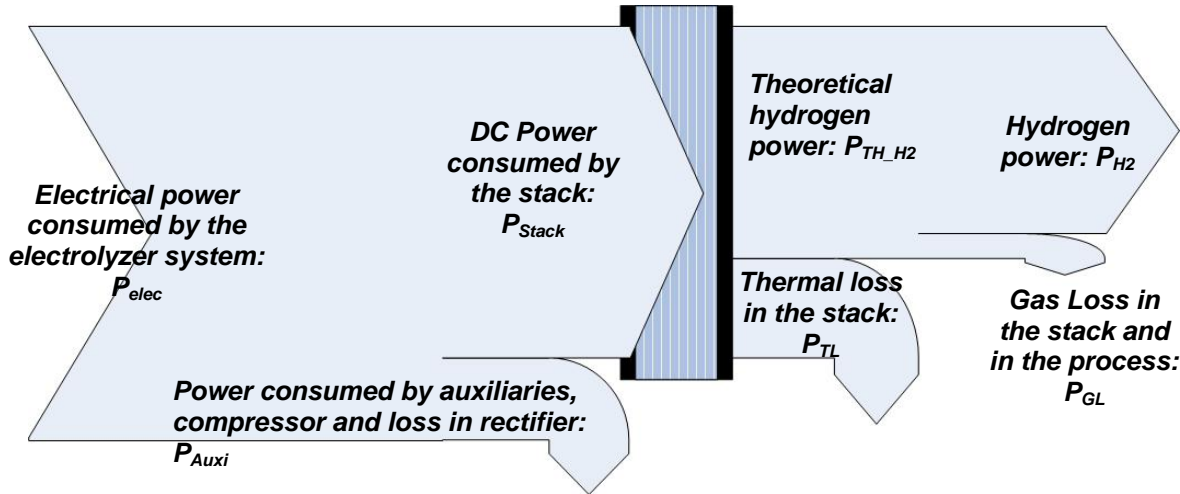


Figure A. 1: Electrolyzer Energy Balance Scheme.

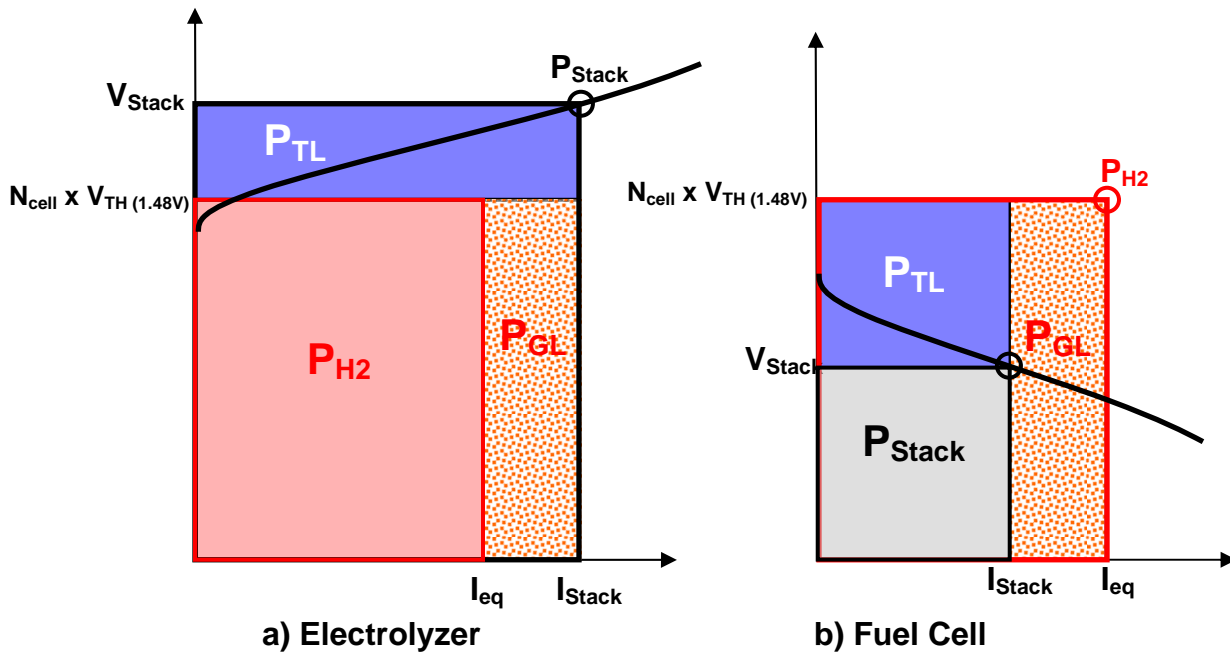
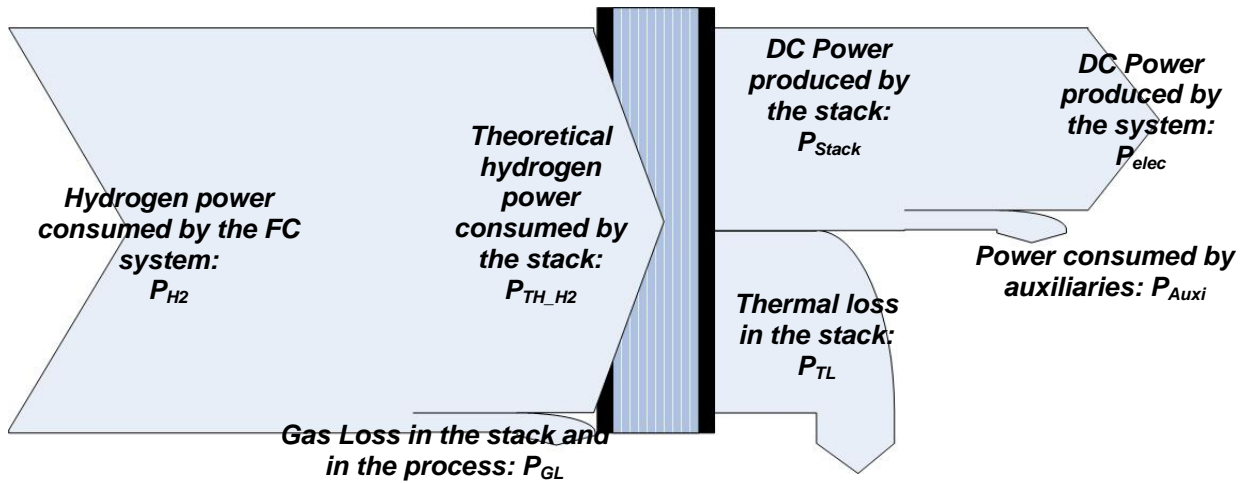


Figure A. 2: Schematic showing gas loss power ( $P_{GL}$ ) and thermal loss power ( $P_{TL}$ ), given the stack current and voltage and the hydrogen flow for a) the electrolyzer and b) the fuel cell.

A similar energy accounting approach is used when analyzing the fuel cell system (Figure A. 3). The fuel cell system consumes hydrogen sent to the stack and produces electricity to supply its auxiliary loads ( $P_{Aux}$ ) and the load demand of the end user ( $P_{elec}$ ). Even if there is hydrogen recirculation in the anode side, the gas efficiency is not 100%. To evaluate the gas loss power, we use equation (2) to calculate the current equivalent,  $I_{eq}$ , to the flow consumed by the system. The right rectangle on Figure A. 2b represents the gas loss power ( $P_{GL}$ ) in the fuel cell system, including gas recombination in the stack

and gas loss in the system. The two other rectangles correspond to the usable electrical power ( $P_{Stack}$ ) and the thermal loss ( $P_{TL}$ ) in the stack.



**Figure A. 3: Steady State Fuel Cell Energy Balance Scheme (without battery).**

All the results presented in this study are expressed as efficiencies (higher heating value basis) and percentage losses. For the electrolyzer, the percentage losses are calculated by dividing the power loss by the AC power supplied to the complete system, whereas the fuel cell percentage losses are calculated by dividing the power loss by the thermal power of hydrogen supplied to the system. All of these terms are defined in Table A. 1, presented on the following page.

**Table A. 1: Definitions of efficiency and loss terms used in the report.**

	<b>Electrolyzer</b>	<b>Fuel Cell</b>
<b>Global equation</b>	$P_{elec} = P_{H_2} + P_{GL} + P_{TL} + P_{Auxi}$	$P_{H_2} = P_{elec} + P_{GL} + P_{TL} + P_{Auxi}$
<b>System efficiency</b>	$P_{H_2} / P_{elec}$	$P_{elec} / P_{H_2}$
<b>Gas Loss</b>	$\frac{P_{GL} / P_{elec} = HHV \times [N_{cell} \times I_{Stack} / (2 \times F) - \dot{n}_{H_2}]}{P_{elec}}$	$\frac{P_{GL} / P_{H_2} = HHV \times [\dot{n}_{H_2} - N_{cell} \times I_{Stack} / (2 \times F)]}{P_{H_2}}$
<b>Thermal Loss</b>	$\frac{P_{TL} / P_{elec} = [P_{Stack} - HHV \times N_{cell} \times I_{Stack} / (2 \times F)]}{P_{elec}}$	$\frac{P_{TL} / P_{H_2} = [HHV \times N_{cell} \times I_{Stack} / (2 \times F) - P_{Stack}]}{P_{H_2}}$
<b>Loss in Auxiliary</b>	$(P_{Auxi} - P_{Compressor}) / P_{elec}$	$P_{Auxi} / P_{H_2}$
<b>Loss in the Compressor</b>	$P_{Compressor} / P_{elec}$	-
<b>Voltage efficiency <math>\eta_v</math></b>	$(N_{Cell} \times 1.48) / V_{Stack}$	$V_{Stack} / (N_{Cell} \times 1.48)$
<b>Gas efficiency* <math>\eta_F</math></b>	$\dot{n}_{H_2} / [N_{Cell} \times I_{Stack} / (2 \times F)]$	$[N_{Cell} \times I_{Stack} / (2 \times F)] / \dot{n}_{H_2}$
<b>Stack efficiency*</b>	$P_{H_2} / P_{Stack} = \eta_v \times \eta_F$	$P_{Stack} / P_{H_2} = \eta_v \times \eta_F$

\* Includes gas loss in the process.